

# Fabrication of Chiral Langmuir–Schaefer Films from Achiral TPPS and Amphiphiles through the Adsorption at the Air/Water Interface

Li Zhang, Qing Lu, and Minghua Liu\*

Lab. of Colloid and Interface Science, Center for Molecular Science, Institute of Chemistry,  
The Chinese Academy of Sciences, 100080, Beijing, People's Republic of China

Received: July 26, 2002; In Final Form: December 6, 2002

Complex monolayer formation between three amphiphiles: cetyltrimethylammonium bromide (CTAB), octadecylamine (ODA), dioctadecyldimethylammonium bromide (DOAB), and tetrakis(4-sulfonatophenyl)porphine (TPPS) at the air/water interface were investigated. It was found that TPPS could form complex monolayers with the amphiphiles at the air/water interface through the electrostatic interaction at pH = 3.1. The complex monolayer could be deposited onto solid substrates using a Langmuir–Schaefer (LS) transfer method to form well-defined LS films. Although TPPS existed as a monomer in aqueous solution at pH 3.1, it could form a J-aggregate in the complex monolayers with the amphiphiles. It is interesting to note that the LS films showed strong split Cotton effect in the circular dichroism (CD) spectra although TPPS and the amphiphiles are all achiral. It was found that only if the chirality of the LS film was related to the J-aggregate formation of TPPS in the LS film, i.e., only when the TPPS formed J-aggregate, can a CD signal be detected. Further investigation through AFM measurements revealed that the nanothread formed in the LS films was responsible for the chirality of the LS film.

## Introduction

Chirality plays an important role in life and material sciences.<sup>1</sup> In biological systems, many molecular recognition processes are needed the match of chirality and thus the different enantiomer of the drugs usually have different effect on the body. In material science, chiral substances are important in modulating the coherence length of materials. While the creation or synthesis of chiral molecules through the auxiliary chiral starting material or chiral catalysts are attracting continues interest, the chirality of supramolecular assemblies is attracting much interesting recently.<sup>2–5</sup> Chiral supramolecular assemblies can not only be formed from component chiral molecules but also from achiral molecules induced by certain chiral substrates.<sup>6–8</sup> In some cases, even those achiral molecules can also form chiral supramolecular assemblies without any chiral template.<sup>9</sup> The appearance of such kind of chirality could be due to the chiral symmetry breakage. So far, the chiral symmetry breakage are usually reported in those systems such as spontaneous precipitation of enantiomorphically enriched sodium chlorate crystals,<sup>10</sup> chiral symmetry breakage in stirred crystallization of super-cooled melt,<sup>11</sup> and the formation of chiral domains in liquid crystals.<sup>12</sup> Also in solution the spontaneous generation of enantiomerically enriched J-aggregates from achiral monomers through stirring the solution had been reported by Hada et al.<sup>13</sup>

Langmuir monolayers at the air/water interface and Langmuir–Blodgett films on solid substrate provide good examples of the precise control of the molecular orientation and packing in two-dimension.<sup>14</sup> Due to this advantage, many molecules can be orderly arranged in the monolayer on water surface. As ordered molecular assemblies, J-aggregate can be easily formed in the monolayers on water surface and these J-aggregates formed in the monolayers can be imprinted into the solid substrates. Using hints from the chirality of the J-aggregate formed in the stirred solution, we intended to see if the

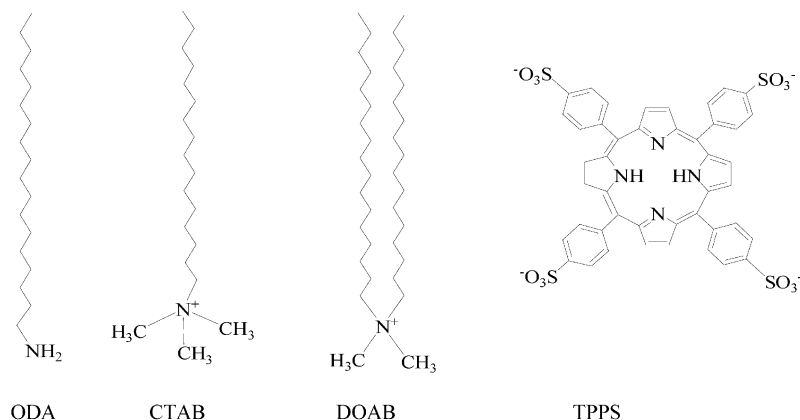
J-aggregate formed in the monolayers on water surface shows the chirality or not.

Tetrakis(4-sulfonatophenyl)porphine (TPPS) is a well-investigated dye. It has a two minus charge and can form stable J-aggregate at an appropriate pH range.<sup>15,16</sup> In solution, it has been reported to form a chiral aggregate under stirring.<sup>17</sup> In this paper, we selected the TPPS as a model compound and investigated their adsorption onto spreading monolayers of oppositely charged amphiphiles at the air/water interface. It has been found that although the TPPS solution did not show aggregation at pH 3.1, when it was adsorbed onto positively charged amphiphilic monolayers of cetyltrimethylammonium bromide (CTAB), octadecylamine (ODA), and dioctadecyldimethylammonium bromide (DOAB), it can form the J-aggregate in the interfacial films. It has been further found that, although both the amphiphiles and TPPS are achiral, the transferred Langmuir–Schaefer (LS) films showed chirality. While there are a lot of papers on the fabrication of chiral LB films using chiral amphiphiles,<sup>18–20</sup> in this paper, we gave one of the fewer reports on the chirality of LS films fabricated from completely achiral molecules. The J-aggregation of TPPS onto amphiphiles monolayers and the chirality of the transferred LS films were characterized by the  $\pi$ -A isotherms, circular dichroism (CD) spectra, X-ray diffraction (XRD), UV–Vis spectroscopy, and atomic force microscopy (AFM) measurements.

## Experimental Section

**Materials.** Cetyltrimethylammonium bromide (CTAB), octadecylamine (ODA), and dioctadecyldimethylammonium bromide (DOAB) were purchased from Aldrich and recrystallized before use. An anionic porphyrin, tetrakis(4-sulfonatophenyl)porphine (TPPS), was purchased from Dojindo Laboratories as a sodium salt and used without further purification. The structures of amphiphiles and TPPS are shown in Scheme 1.

## SCHEME 1



**Procedures.** The surface pressure ( $\pi$ )–molecular area ( $A$ ) isotherms were measured on a KSV minitrough (KSV 1100, Helsinki, Finland). To fabricate the complex monolayers between the amphiphiles and TPPS, a chloroform solution of CTAB, ODA, and DOAB (ca. 1 mM) were spread on an aqueous solution containing  $1 \times 10^{-5}$  M TPPS. The pH of the subphase was adjusted to 3.1 using hydrochloric acid to avoid the aggregation of TPPS. After 10 min of evaporation of the solvent, surface pressure–area isotherms were recorded by compressing the barrier at a constant speed of 5 mm/min.

The complex monolayers were transferred onto quartz substrates using a horizontal lifting method for UV–vis, CD, and XRD measurements. A JASCO UV-530 spectrophotometer was used for the polarized UV–vis absorption measurements and a polarizer (Hitachi Mode 650-0155) was placed in front of the LS films. CD spectra were recorded on a JASCO J-810 CD spectrometer and X-ray diffraction (XRD) was performed on a RIGAKU X-ray diffractometer (D/Max-RB) with Cu K $\alpha$  radiation.

To measure the AFM of the transferred films, a freshly cleaved mica was used and AFM was recorded on a Seiko Instrument SPA 400 Multimode system (Japan) with a SI-DF20 silicon cantilever (resonance frequency 138 kHz, spring constant 16 N/m) using the tapping mode.

## Result and Discussion

### Monolayer Characteristics at the Air–Water Interface.

Figure 1 shows the surface pressure–area ( $\pi$ – $A$ ) isotherms of CTAB, DOAB, ODA monolayers spread on the aqueous subphase containing  $1 \times 10^{-5}$  M TPPS. Stable monolayers are formed in any case. In comparison with the monolayers of the compounds on the pure water surface, enlargements of the

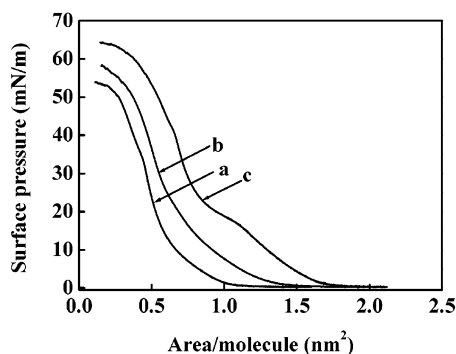


**Figure 1.** The surface pressure–area isotherms of the monolayers of (a) ODA, (b) CTAB, and (c) DOAB on the subphase containing TPPS at pH 3.1 at 20 °C.

molecular areas are observed for that on TPPS subphase. This indicates that there exists a strong interaction between the amphiphiles in monolayer and TPPS in the subphase. Due to the fact that CTAB and DOAB are positively charged and ODA is also positively charged at pH = 3.1,<sup>21</sup> TPPS has a negative charge, it is reasonable to think that electrostatic interaction contributed mainly to such an interaction. The limiting area of ODA on pure water at pH 3.1 was about 0.22 nm<sup>2</sup>/molecule.<sup>22</sup> The molecular area extrapolating from the isotherm on TPPS subphase was increased to 0.72 nm<sup>2</sup>/molecule. According to the CPK model, a TPPS molecule could be regarded as a square, and the length of the side is ca. 1.3 nm.<sup>23</sup> Therefore, it could be regarded that in the complex monolayers of ODA and TPPS, the macrocyclic ring of the TPPS molecule is inclined to the plane of the complex monolayer. A similar conclusion could be drawn on the other complex monolayers of CTAB/TPPS and DOAB/TPPS.

**UV–Vis Absorption Spectra of the LS Films and the Orientation of TPPS in the Complex Films.** The complex monolayers of the amphiphiles and TPPS could be transferred onto solid substrate. Figure 2 shows the UV–vis spectra of the transferred LS film in comparison with TPPS in subphase (pH 3.1). In the aqueous solution, TPPS showed two adsorption bands at 432 nm and 640 nm, which are attributed to the Soret band and Q-band, respectively. In the LS film, Soret and Q-bands are observed at 490 and 709 nm, respectively, which showed a large red shift in comparison with those in aqueous solution. These large red-shifted bands can be ascribed to the formation of J-aggregate of TPPS in the complex LS films. In addition, a relative weak absorption band could be observed in the LS films in 422 nm, which is blue shifted in comparisons

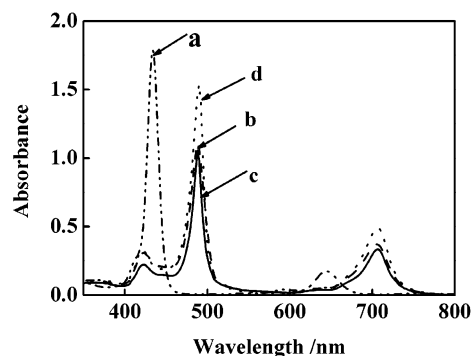


**Figure 2.** UV–Vis spectra of (a, dash dotted line) the solution of TPPS and 20-layer LS films of amphiphiles (b, dash line) ODA, (c, solid line) CTAB, and (d, dotted line) DOAB with TPPS transferred at 30 mN/m.

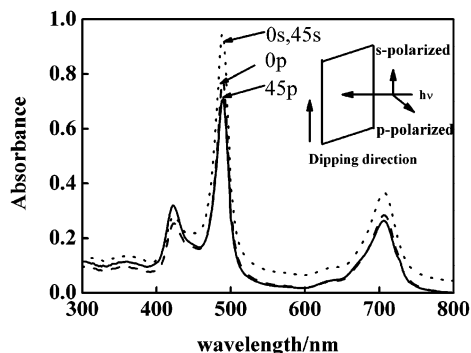


**Figure 3.** Polarized UV–vis spectra of complex film of ODA/TPPS. The inset in this figure indicates the geometrical definitions.

with the TPPS solution. This band can be attributed to the formation of H-aggregate.<sup>24</sup> Therefore, upon complex formation between the amphiphiles monolayer and TPPS at the air/water interface through the electrostatic interaction, TPPS can be incorporated into the LS film as a J-aggregate or H-aggregate.

On the other hand, absorption band was not influenced by the surface pressure, i.e., those LS films transferred at lower or higher surface pressure show similar UV–vis spectra. This indicated that the aggregation can be realized both at lower and higher surface pressure. The pH of the subphase affected the aggregation of TPPS in complex monolayers also. When the amphiphiles spread on the TPPS subphase with pH 5.0, no J-aggregate was obtained. This was due to the fact that porphyrin  $H_2TPPS^{4-}$  has a  $pK_a$  of about 4.9,<sup>15</sup> and it could not form J-aggregate at this pH.

The UV–vis absorption spectrum of TPPS in LS film is sensitive to the direction of polarization of an incident light, which enables the use of polarized light to probe the orientation of TPPS molecule in LS films. The ratio of the absorbance for s-polarized light to p-polarized light,  $A_s/A_p$ , directly relates to the angular distribution of the transition dipoles in multilayer assemblies. The ratio reveals the chromophore orientation of TPPS in LS films. For porphyrin molecules, the two transition dipoles lie in the molecular plane at an angle of  $90^\circ$  along the axis through the pyrrole nitrogen at opposite positions. The polarization direction of the  $\pi-\pi^*$  Soret band is parallel to the molecular plane. To estimate the average tilted angle of the TPPS, polarized UV–vis spectra of the complex LS films were measured on the quartz plates at incidence angles of  $0^\circ$  and  $45^\circ$  in the s- or p-polarized light. Figure 3 shows an example of the polarized UV–vis spectra for ODA/TPPS LS films. The dichroic ratio of  $A_s/A_p$  are listed for all the LS films. According to Yoneyama's equation<sup>25</sup> and assuming the refractive index  $n$  of the films is 1.5, the angle between the porphyrin macrocyclic plane in the LS films and the quartz substrate was estimated to be  $40.5^\circ$ ,  $41.5^\circ$  and  $44.9^\circ$  for the complex film of CTAB/TPPS, ODA/TPPS, and DOAB/TPPS, respectively, supporting the above J-aggregation of TPPS in the complex films.

$$\cos^2 \theta = \frac{D_0 - (1 + \sin^2 \beta)D_{45}}{(1 - 2 \sin^2 \beta)D_{45} - (1 + D_{45} \sin^2 \beta)D_0}$$

where  $\theta$  is the angle between the macrocyclic plane of porphyrin and the substrate,  $\beta = \sin^{-1}(n_1 \sin \beta'/n_2)$ ,  $\beta'$  is the incident angle, and  $n_1$  and  $n_2$  are the refractive index of the air and film, respectively.  $D_0$  and  $D_{45}$  were the dichroic ratio,  $A_s/A_p$ , at  $0^\circ$  and  $45^\circ$ , respectively (see Table 1).

**XRD Measurement.** To investigate the layer structure of the LS films, X-ray diffractions were measured on the transferred

**TABLE 1: Ratios of the s-Polarized to p-Polarized Absorbance of the Soret Band in the UV–Vis Spectra of the Complex Films at Incidence Angles of  $0^\circ$  and  $45^\circ$**

LS films	$A_s/A_p$		$\theta$ (deg)
	( $\beta' = 0^\circ$ )	( $\beta' = 45^\circ$ )	
ODA/TPPS	1.22	1.33	41.5
CTAB/TPPS	1.23	1.35	40.5
DOAB/TPPS	0.95	1.03	44.9

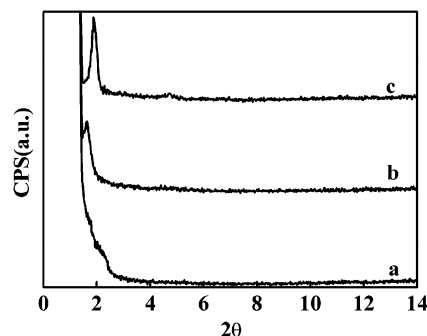
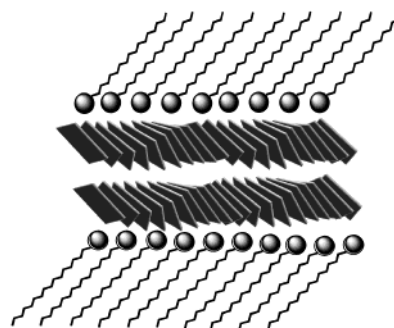


**Figure 4.** XRD diffraction of the 20-layer complex LS films of amphiphiles, (a) ODA, (b) DOAB, and (c) CTAB on the subphase containing TPPS.

## SCHEME 2



complex LS films. Figure 4 shows the X-ray diffraction patterns of the 20-layer LS films transferred from the amphiphiles monolayers on TPPS solution surface. Bragg diffraction peaks were observed for the complex LS films of CTAB/TPPS and DOAB/TPPS, while only a broad shoulder was observed in the case of ODA/TPPS film. This indicates that the complex LS film of ODA/TPPS is less ordered. From the Bragg's equation  $2D \sin \theta = n\lambda$ , the layer distances of the LS films of CTAB/TPPS and DOAB/TPPS can be calculated as 4.69 and 5.45 nm, respectively. Using the CPK model, the length of CTAB and DOAB molecular in fully stretched conformation are estimated as 2.1 and 2.5 nm, respectively. Considering the above polarized UV–vis spectra concerned with the orientation of TPPS macrocyclic ring, it could be regarded that a Y-type complex film are formed, in which both the alkyl chain of the amphiphiles and the macrocyclic ring of TPPS are rather tilted, as shown in Scheme 2.

**Chirality of the Transferred LS Films.** It is reported that J-aggregate of TPPS can show chirality in solution.<sup>26</sup> It is interesting to note that the complex LS films of amphiphiles and TPPS showed also chirality. In the case of LS films, the CD signal can be affected by the linear dichroism (LD).<sup>27–29</sup> To get rid of the influence of the LD, the LS film was placed in different angles and an average was taken as in the case of those reported in the literature.<sup>28,29</sup> Further, it is found that if



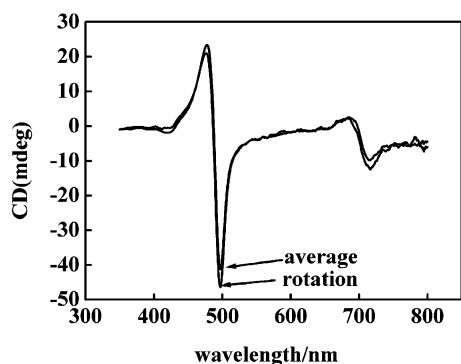


**Figure 5.** Comparison between the CD spectra of 20-layer LS films of ODA with TPPS obtained by averaging the CD spectrum in eight different rotation angles (0, 45, 90, 135, 180, 225, 270, 315, and 360) and that obtained by continuous rotation.

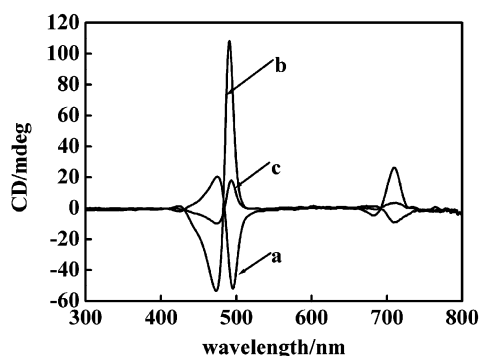


**Figure 6.** CD spectra of 20-layer LS films of (a) ODA, (b) CTAB, and (c) DOAB with TPPS transferred at 30 mN/m.

the film is rotated in the film plane, LD could be clearly rid of the CD spectra averaged at eight different angles (0, 45, 90, 135, 180, 225, 270, 315, and 360), which are the same as those obtained in a rotating manner, as shown for example in Figure 5. The CD spectra reported below are obtained by rotating the film during the measurement.

Figure 6 shows that the CD spectra of LS film transferred onto the solid substrate at a surface pressure of 30 mN/m. The remarkable bisignate (with both positive and negative sign) CD signals centered at the absorption wavelength of the J-band at 490 nm and the same symbolic bisignate CD signals centered at 709 nm are observed. Some important features are obtained

concerning the CD measurement. First, although we did not detect any CD signals in the TPPS solution, strong CD signals are observed in all the LS films. Second, we have found that the CD signal could be detected only when J-aggregate was formed. We have transferred LS films on a subphase with pH 5.0, where TPPS did not form a J-aggregate even in the complex film, no CD signal was detected. Third, the sign of the CD signal was randomly appeared, i.e., it could be either positive or negative in different deposition batch although a CD signal was certainly appeared. Fourth, the strength of the CD signal is not necessarily linear to the UV-vis absorption. For example, in the UV-vis spectra, DOAB/TPPS LS film shows the strongest absorption in J-band. However, the CD signal in the CD spectra is the weakest among the three films.

These CD features clearly indicated that the complex films are chiral although both TPPS and the amphiphiles are achiral. The random appearance of the CD signal excluded out the existence of any chiral impurity in the LS films. The fact that CD signals are only detected in the J-aggregate clearly indicates that the chirality of the LS film comes from the J-aggregate of the TPPS in the LS film.

It was shown that the J-aggregates of TPPS or cyanine dye could show chirality by physical stirring or chemical induction with chiral polymeric templates. In our work, there is neither physical force nor chiral chemical inducement. The chirality of the film is formed spontaneously. Such spontaneously formed chirality may be due to the helical (right or left-hand) alignment of the molecular plane.<sup>30</sup> It is well-known that in typical J-aggregate, the TPPS molecules are stacked head to tail just like a linear "polymer". If the molecular planes distorted in a certain degree in one direction, then a chiral J-aggregate could be formed. Generally, the chance to form the right-helical and left-helical should be the same and only racemic aggregate could be obtained. However, the symmetry could be broken in certain conditions such as chemical reaction, stirred crystallization of super cooled melt and stirred aggregation of dyes. In the present case, it seems that a simple air/water interface could also afford the symmetry breakage of the achiral molecules to form a chiral aggregated.

**AFM Picture.** To confirm the above suggestion of the chirality of the LS films, we have measured the surface morphologies of the LS films using AFM. Figure 7 shows the AFM pictures of one layer LS film on a freshly cleaved mica surface. In CTAB/TPPS monolayer, a long threadlike structure

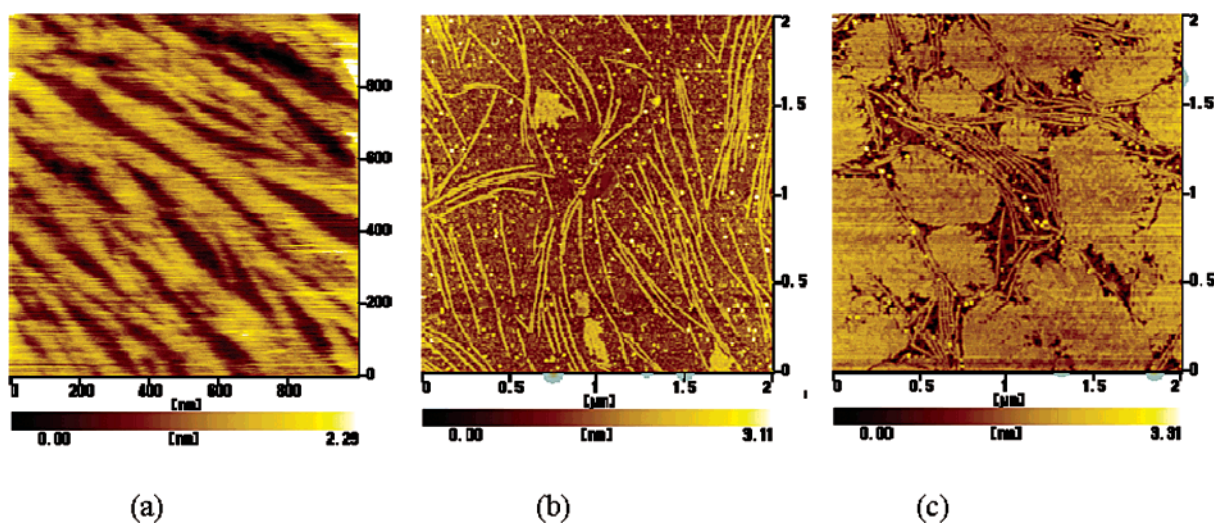


**Figure 7.** The AFM picture of complex LS films of (a) ODA, (b) CTAB, and (c) DOAB with TPPS.

was observed at the whole scale of  $2\mu\text{m}$ . The thread is about several tens of nanometers in width and extended to several hundreds nanometers. Similar thread morphologies are observed in the other monolayers. In the case of DOAB/TPPS monolayer, the thread is embedded in a large flat domain, while in the case of ODA/TPPS, the thread gathered around the stripe. In related to the above CD spectra, it can be suggested that it is such nanothread that contributed to the chirality of the LS films and the amount of the threadlike domain seems to be in proportion with the intensity of the CD signals. This explains why in the CD measurement the absorption intensity of the J band is not necessarily linear to the CD intensity. In the case of DOAB, relative weak CD signal was observed although strong absorption of the J-aggregate was observed in the UV–vis spectra. This is because, in DOAB/TPPS film, only a small amount of thread was detected.

It should be further noted that three amphiphiles are different in their headgroups and hydrophobic tail and the chirality of the formed LS films are different. Due to the double hydrophobic tail or a relative small headgroup, both ODA and DOAB could form more densely packed monolayers when interacting with TPPS. It is interesting to note the dihedral angle between the film plane and the macrocyclic ring increased in the order of CTAB/TPPS, ODA/TPPS, and DOAB/TPPS LS films, while the intensity of the CD signals decreased in the same order. It is well-known that when the dihedral angle is below  $54.7^\circ$ ,<sup>31</sup> it forms a J-aggregate. Although we got the same absorption band in UV–vis spectra of the LS films, the subtle tilt angle of TPPS was different. The value of the angles seems to be related to the coherent length of the chirality, i.e., the small dihedral angle can afford larger aggregate and shows strong CD signal.

## Conclusions

Complex monolayers between TPPS and amphiphiles monolayers can be formed at the air/water interface through the electrostatic interaction. The complex monolayers can be transferred onto solid substrate using the Langmuir–Schaefer method to form ordered LS films in which TPPS assembled as a J-aggregate although it did not aggregate in solution. The LS films showed chirality although both TPPS and the amphiphiles are achiral. The chirality of the complex LS films is due to the formation of chiral J-aggregate of TPPS. Although the chance of TPPS to form right-hand and left-handed chiral J-aggregate are equal, the balance can be broken in the surface monolayer formation and/or during the film transfer and thus resulted in the chiral LS films. It is further confirmed that the threadlike structure formed in the film is responsible for the chirality of the films.

**Acknowledgment.** This work was supported by the Outstanding Youth Fund No. 20025312, National Natural Science Foundation of China Nos. 29992583 and 20273078, the Major State Basic Research Development Program (Nos. G2000078103 and 2002CCA03100), and the Fund of the Chinese Academy of Sciences.

## References and Notes

- (1) Berova, N.; Nakanishi, K.; Woody, R. W. *Circular Dichroism Principles and Applications*, 2nd ed.; Wiley-VCH: New York, 2000.
- (2) Wang, M. M.; Silva, G. L.; Armitage, B. A. *J. Am. Chem. Soc.* **2000**, *122*, 9977.
- (3) Yashima, E.; Maeda, K.; Okamoto, Y. *Nature* **1999**, *399*, 449.
- (4) Oda, R.; Huc, I.; Schmutz, M.; Candau, S. J.; MacKintosh, F. C. *Nature* **1999**, *399*, 566.
- (5) Prins, L. J.; Jong, D. F.; Timmerman, P.; Reinhoudt, D. N. *Nature* **2000**, *408*, 181.
- (6) Kawasaki, T.; Tokuhito, M.; Kimizuka, N.; Kunitake, T. *J. Am. Chem. Soc.* **2001**, *123*, 6792.
- (7) Bellacchio, E.; Lauceri, R.; Gurrieri, S.; Monsù Scolaro, L.; Romeo, A.; Purrello, R. *J. Am. Chem. Soc.* **1998**, *120*, 12353. (b) Lauceri, R.; Raudino, A.; Monsù Scolaro, L.; Micali, N.; Purrello, R. *J. Am. Chem. Soc.* **2002**, *124*, 894. (c) Purrello, R.; Raudino, A.; Monsù Scolaro, L.; Loisi, A.; Bellacchio, E.; Lauceri, R. *J. Phys. Chem. B* **2000**, *104*, 10900.
- (8) Chowdhury, A.; Wachsmann-Hogiu, S.; Bangal, P. R.; Raheem, I.; Peteanu, L. A. *J. Phys. Chem. B* **2001**, *105*, 12196.
- (9) Rossi, U. D.; Dähne, S.; Meskers, S. C. J.; Dekkers, H. P. J. M. *Angew. Chem., Int. Ed. Engl.* **1996**, *35*, 760.
- (10) Kondepudi, D. K.; Kaufman, R. J.; Siggh, N. *Science* **1990**, *250*, 975. (b) Kondepudi, D. K.; Bullock, K. L.; Digits, J. A.; Hall, J. K.; Miller, J. M. *J. Am. Chem. Soc.* **1993**, *115*, 10211.
- (11) Kondepudi, D. K.; Laudadio, J.; Asakura, K. *J. Am. Chem. Soc.* **1999**, *121*, 1448.
- (12) Link, D. R.; Natale, G.; Shao, R.; MacLennan, J. E.; Clark, N. A.; Körblová, E.; Walba, D. M. *Science* **1997**, *278*, 1924.
- (13) Honda, C.; Hada, H. *Tetrahedron Lett* **1976**, *177*. (b) Honda, C.; Hada, H. *Photogr. Sci. Eng.* **1977**, *21*, 91.
- (14) Gaines, G. L., Jr. *Insoluble monolayers at Liquid–Gas Interfaces*; Interscience: New York, 1966.
- (15) Maiti, N. C.; Ravikanth, M.; Mazumdar, S.; Periasamy, N. *J. Phys. Chem.* **1995**, *99*, 17912.
- (16) Micali, N.; Mallamace, F.; Romeo, A.; Purrello, R.; Monsù Scolaro, L. *J. Phys. Chem. B* **2000**, *104*, 5897. (b) Micali, N.; Romeo, A.; Lauceri, R.; Purrello, R.; Mallamace, F.; Monsù Scolaro, L. *J. Phys. Chem. B* **2000**, *104*, 9416.
- (17) Ribó, J. M.; Crusats, J.; Sagués, F.; Claret, J.; Rubires, R. *Science* **2001**, *292*, 2063.
- (18) Arnett, E. M.; Harvey, N. G.; Rose, P. L. *Acc. Chem. Res.* **1989**, *22*, 131. (b) Harvey, N. G.; Mirajovsky, D.; Rose, P. L.; Verbiar, R.; Arnett, E. M. *J. Am. Chem. Soc.* **1989**, *111*, 1115. (c) Heath, J. G.; Arnett, E. M. *J. Am. Chem. Soc.* **1992**, *114*, 4500.
- (19) Nuckolls, C.; Katz, T. J.; Verbiest, T.; Elshocht, S. V.; Kuball, H.-G.; Kiesewalter, S.; Lovinger, A. J.; Persoons, A. *J. Am. Chem. Soc.* **1998**, *120*, 8656.
- (20) Feng, F.; Miyashita, T.; Okubo, H.; Yamaguchi, M. *J. Am. Chem. Soc.* **1998**, *120*, 10166.
- (21) Betts, J. J.; Pethica, B. A. *Trans. Faraday Soc.* **1956**, *52*, 1581.
- (22) Ray, K.; Nakahara, H. *J. Phys. Chem. B* **2002**, *106*, 92.
- (23) Ariga, K.; Lvov, Y.; Kunitake, T. *J. Am. Chem. Soc.* **1997**, *119*, 2224.
- (24) Ribó, J. M.; Crusats, J.; Farrera, J. A.; Valero, M. L. *J. Chem. Soc. Chem. Commun.* **1994**, 681.
- (25) Yoneyama, M.; Sugi, M.; Saito, M. *Jpn. J. Appl. Phys.* **1985**, *25*, 961.
- (26) Maiti, N. C.; Mazumdar, S.; Periasamy, N. *J. Phys. Chem. B* **1998**, *102*, 1528.
- (27) Norden, B. *J. Phys. Chem.* **1977**, *81*, 151.
- (28) Saeva, F. D.; Olin, G. R.; *J. Am. Chem. Soc.* **1977**, *99*, 4848.
- (29) Spitz, C.; Dähne, S.; Ouart, A.; Abraham, H.-W. *J. Phys. Chem. B* **2000**, *104*, 8664.
- (30) Berlepsch, H. V.; Böttcher, C.; Ouart, A.; Burger, C.; Dähne, S.; Kirstein, S. *J. Phys. Chem. B* **2000**, *104*, 5255. (b) Berlepsch, H. V.; Böttcher, C.; Ouart, A.; Regenbrecht, M.; Akari, S.; Keiderling, U.; Schnablegger, H.; Dähne, S.; Kirstein, S. *Langmuir* **2000**, *16*, 5908. (c) Kirstein, S.; Berlepsch, H. V.; Böttcher, C.; Burger, C.; Ouart, A.; Reck, G.; Dähne, S. *Chem. Phys. Chem.* **2000**, *3*, 146.
- (31) Osburn, E. J.; Chau, L.-K.; Chen, S.-Y.; Collins, N.; O'Brien, D. F.; Armstrong, N. R. *Langmuir* **1996**, *12*, 4784.